

**T11 - Neutron Diffraction****T11 - P201****MEASUREMENT OF NEUTRON POWDER DIFFRACTION FOR HIGHLY NEUTRON ABSORBING SPECIMENS****Yong Nam Choi, Baek-Seok Seong, Chang-Hee Lee and Young Jin Kim***HANARO Center, Korea Atomic Energy Research Institute, Yuseong, Daejeon 305-600, Korea*

Neutron scattering would be more useful than x-ray scattering for the study of bulk properties of materials because it has very high penetration property. It means that the interaction strength between the neutron and a matter is very weak and thus a lot of sample amount and measurement time are necessary in general. But if the amount of sample is much enough, one can use this property as an advantage because one does not have to be thoughtful of sample geometry and alignment. Neutron scattering has strong advantage for the structural study of materials containing light and heavy elements, adjacent elements or isotopes since the neutron scattering length of an element which represents the interaction strength does not depend on the atomic number. However some elements such as Gd, Sm, Eu, Cd and B have very high neutron absorption cross-section which gives us serious limitation on measurement.

In the neutron powder diffraction experiment, samples are usually prepared in a thin cylindrical vanadium container. The typical diameter of the cylinder ranges from a few mm up to about 15 mm. If the amount of the sample is much enough and the neutron absorption by the sample is small enough, the signal intensity is generally proportional to the volume of the sample or to the square of the cylinder diameter. However, if the absorption is not negligible, the scattering intensity does not monotonically depend on the amount of sample. The scattering intensity from a neutron

absorbing material is proportional to (sample amount)  $\exp(-\mu x)$ , where  $\mu$  is the linear attenuation factor of the material and  $x$  is the path length and thus there exist the optimum condition of sample preparation which gives us maximum signal intensity.

There are three methods of sample preparation to overcome the high attenuation problem. One of them is the dilution method which reduce the effective density of the sample and hence reduce the value of the linear attenuation factor ( $\mu$ ) by mixing with well known powders such as aluminum or vanadium. Another one is the contraction method which decrease the path length ( $x$ ) by using a shell type sample container. The last one is the simultaneous usage of the two methods, dilution+contraction.

Analytic calculation of the general form of the neutron transmission ( $I/I_0$ ) as a function of control parameters (the dilution ratio and the dimension of sample container) and scattering angle ( $\theta$ ) is impossible but we could calculate for some special cases. We have tried to measure for very highly absorbing specimens by considering the calculated results and obtained quite reasonable intensities. Details of the calculation and experimental results will be presented. And a selection criteria according to the degree of neutron attenuation or absorption by sample will also be suggested.

**T11 - P202****INDUSTRIALLY ORIENTED IN-SITU NEUTRON DIFFRACTION: DEVELOPMENT OF A MEDIUM PRESSURE GAS CYCLING CELL****Lachlan Cranswick***NRC, Building 459, Station 18, CRL, Chalk River, Canada*

Diffraction measurements of industrial and scientifically relevant materials under room temperature conditions can miss important information obtainable by measuring at non-ambient conditions of temperature, pressure and atmosphere. However, the poor penetrating power of standard laboratory X-rays can make many types of in-situ experiment impractical. Due to their penetrating power, both neutron diffraction and synchrotron based energy dispersive diffraction offer opportunities to understand scientific and industrial processes by performing in-situ equipments in specially made ancillary equipment. The main limitation is

the design and construction of appropriate ancillary equipment to make goodly use of the neutrons or X-rays. In a neutron example, this poster will elaborate on a new computer controlled gas cycling cell, of 3 gases (deuterium, hydrogen and helium purge gas) into a sample cell using mass flow controllers, being constructed at the neutron scattering facilities in Chalk River, Ontario, Canada. Initially designed to go up to 10 bar gas pressure, a 50 bar gas pressure sequel is planned using the experience gained constructing the 10 bar version.



T11 - P203

## THE CRYSTAL STRUCTURE OF DEFECTIVE STANNITE $Zn_{1-x}Mn_xGa_2Se_4$ ( $0 < x < 0.5$ ) INVESTIGATED BY NEUTRON POWDER DIFFRACTION

M.C. Morón<sup>1</sup> and S. Hull<sup>2</sup>

<sup>1</sup>Instituto de Ciencia de Materiales de Aragón, Univ. Zaragoza – C.S.I.C. (Spain), nina@unizar.es.

<sup>2</sup>ISIS Facility, Rutherford Appleton Laboratory (UK), s.hull@rl.ac.uk.

Diluted magnetic semiconductors (DMSs) combine two areas of research: semiconductors and diluted magnetism. Thus DMSs include charge and spin variables in a single material. The science based on their interaction and resulting multifunctionality has attracted significant attention [1].  $ZnGa_2Se_4$  and  $MnGa_2Se_4$  are semiconductors showing direct gaps at around 2.3 and 2.5 eV, respectively [2].  $Mn^{2+}$  is a magnetic ion with spin  $S = 5/2$ . The controlled substitution of Zn ions by Mn in the  $ZnGa_2Se_4$  matrix gives the series of DMSs  $Zn_{1-x}Mn_xGa_2Se_4$ .

Orange single crystals of  $Zn_{1-x}Mn_xGa_2Se_4$  with  $x = 0.00, 0.104(4), 0.240(4), 0.343(4)$  and  $0.482(4)$  were synthesized using the chemical vapour transport method. The Mn concentration  $x$  was obtained from powder diffraction and magnetic experiments. Room temperature time-of-flight neutron diffraction data were collected in the range  $0.8 < \lambda < 3.2$  on the powder diffractometer Polaris at the ISIS source, UK.

$ZnGa_2Se_4$  crystallizes in the tetragonal space group I-42m exhibiting a defective stannite structure with  $a = 5.5117(3)$  Å and  $c = 10.9643(6)$  Å [3]. The cations are surrounded by a tetrahedral environment of four Se atoms. The crystal structure exhibits a random disorder affecting the Zn and half of the Ga atoms. The other end member of the  $Zn_{1-x}Mn_xGa_2Se_4$  series is  $MnGa_2Se_4$ . The crystal structure of this semiconducting magnetic material is rather similar to that reported for the Zn derivative. The structural arrangement of the atoms corresponds to a defective chalcopyrite structure, tetragonal space group I-4, with  $a = 5.677(1)$  Å and  $c = 10.761(2)$  Å [4]. A significant difference between the crystal structure of both end members of the series is that there is no cation disorder in  $MnGa_2Se_4$ .

The crystal structure of  $Zn_{1-x}Mn_xGa_2Se_4$  with  $x = 0.00, 0.104(4), 0.240(4), 0.343(4)$  and  $0.482(4)$  has been refined by using the Rietveld method. The structural arrangement of atoms in  $ZnGa_2Se_4$  has been used as the starting model. Crystal symmetry, space group, unit cell parameters,

atomic positions, distribution of magnetic ions and isotropic temperature factors have been calculated together with main bond distances and angles. The neutron powder diffraction data show that all the materials under study keep the symmetry of the Zn derivative. All of them crystallize in the space group I-42m.

The evolution of the tetragonal parameters  $a$  and  $c$  with  $x$  is dissimilar in  $Zn_{1-x}Mn_xGa_2Se_4$   $0 < x < 0.5$ . While  $a$  increases with the Mn content,  $c$  remains essentially constant. There is a decrease of  $c/a$  with  $x$ , which would suggest a tendency to an augmentation of cation ordering as the Mn content increases [5]. One interesting point is the arrangement of the magnetic cations since they could be randomly distributed as for the Zn ions in  $ZnGa_2Se_4$  or ordered as in  $MnGa_2Se_4$ . Manganese is clearly differentiated by the neutron diffraction technique due to its negative coherent neutron scattering length. The Rietveld refinements show that the Mn atoms are disordered, sharing crystallographic position (4d) with the Zn ions and half of the Ga atoms. Therefore the lattice site available to the magnetic cations is not the same in  $MnGa_2Se_4$  (2d) as in  $Zn_{1-x}Mn_xGa_2Se_4$   $0 < x < 0.5$  (4d). This fact notably influences the magnetic properties of the system. They differ significantly from those expected for the classical dilution of a magnetic semiconductor.

- [1] M. Averous and M. Balkanski, *Semimagnetic Semiconductors and Diluted Magnetic Semiconductors* (Plenum Press, New York, 1991); W. Zaets and K. Ando, *Appl. Phys. Lett.* 77 (2000) 1593.
- [2] A. Millán and M. C. Morón, *J. Appl. Phys.* 89 (2001) 1687.
- [3] T. Hanada, F. Izumi, Y. Nakamura, O. Nittono, Q. Huang and A. Santoro, *Physica B* 241-243 (1998) 373.
- [4] M. Cannas, L. Garbato, A. G. Lehmann, N. Lampis and F. Ledda, *Cryst. Res. Technol.* 33 (1998) 417.
- [5] L. Gastaldi, M. G. Simeone and S. Viticoli, *Solid State Commun.* 55 (1985) 605.

T11 - P204

## DISTRIBUTION OF CATIONS IN CHEMISORBED ZEOLITIC CATALYSTS BY NEUTRON DIFFRACTION

S. Vratislav<sup>1</sup>, M. Dlouhá<sup>1</sup>, V. Bosáček<sup>2</sup>

<sup>1</sup>Czech Technical University, Faculty of Nuclear Sciences and Physical Engineering, Department of Solid State Engineering, Břehová 7, 115 19 Prague 1, Czech Republic

<sup>2</sup>J. Heyrovský Institute of Physical Chemistry, 182 23 Prague 8, Czech Republic  
vratisla@jffi.cvut.cz

Continuous interest in the structure investigation of zeolites is stimulated by their potential practical use in the chemical technology. Zeolites exhibiting regular structure which can be easily modified are important candidates for this type catalyst and many laboratories try therefore to „tailor“ zeolitic catalysts of the requested properties in oxygen atoms of the faujasite framework. Nature of acid or basic sites and the distribution of sodium cations and chemisorbed methyl groups in the zeolitic lattice belong to the most important problems of surface chemistry. Theoretical investigations [1] demonstrated that chemical properties of protons are controlled by actual basicity of the lattice oxygen atoms and by the character of bonds where protons are attached. Experimental support was obtained also from the results of diffraction methods, where namely neutron diffraction provided direct evidence on the location of protons in faujasites with various H<sup>+</sup>/Na<sup>+</sup> ratio [2]. The aim of our study was to estimate the location of chemisorbed species in the lattice and to elucidate the role

and participation of various lattice oxygen types in chemisorption of methyl cations. We have made an attempt to estimate regular distribution of cations and chemisorbed species over the lattice and to locate chemisorbed CH<sub>3</sub><sup>+</sup> ions at different oxygen atoms.

Well-developed crystals of NaY, NaX and NaLSX with high content of sodium cations and with low content of defects and decationation were used in this study. The reaction of methyl iodide with sodium cations was used for the preparation of anchored methyl groups in the structure of zeolites (and controlled by <sup>13</sup>C MAS NMR spectra were measured). Neutron powder diffraction patterns were collected at temperature of 298 and 7 K on the KSN-2 diffractometer, which is placed at the LVR-15 research reactor in Řež near Prague. The complete structural parameters were determined by Rietveld analysis of powder neutron diffraction data using the GSAS software package.

Our structural parameters for the initial dehydrated bare samples and parameters for characteristic chemisorbed

**Table 1.** Cationic Sites in Dehydrated Faujasites NaX and NaLSX

Zeolite	Cation Site	Type	Hunger <sup>1)</sup> et al. *)	Grey <sup>2)</sup> et al. *)	Olson <sup>3)</sup> **)	Plevert <sup>4)</sup> et al. **)	Vratislav et al. ***)
NaX	SI	16c	4	2	3		3
	SI'	32e	16	28	29		29
	SII	32e	32	32	31		31
	SIII'(1,2)	96g	25	13	21		21
	SIII'(3)	96g	6	10	8		9
NaLSX	SI	16c	4			0	0
	SI'	32e	18			32	25
	SII	32e	32			32	32
	SIII'(1,2)	96g	26			16	34
	SIII'(3)	96g	13			15	8

Remarks: \*) NMR results, \*\*) X-ray diffraction, \*\*\*) neutron diffraction, our study

1) Solid State Nucl. Magn. Reson. 6 (1996) 1-6, 2) J. Am. Chem. Soc. 119 (1997) 1981-89 3) Zeolites 15 (1995) 439-443, 4) J. Phys. Chem. B 101(1997) 10340-46



NaX and NaLSX samples are given in [3,4]. The occupation numbers of cations (Tab. 1) and the location of CD<sub>3</sub> groups were determined by means of difference Fourier maps. Zeolite LSX (low silica X) has a Si/Al ratio of 1 and represents the highest number of charge-compensating cations among all faujasites. Parameters of NaLSX given in [4] were refined in both recently discussed space groups, as in Fd-3 space group as in Fddd (orthorhombic) group but without any significant difference.

Cations are distributed over six possible sites in the frame of Fd3 space group. Our experimental data allow to compare the changes in the occupation of positions of the Na cations in original evacuated NaX and in the same sample after chemisorption of methyl iodide. The occupation numbers of Na cations in chemisorbed NaX has been decreased for S<sub>I'</sub> and S<sub>I''</sub> in contrary to the increase for S<sub>III</sub> in comparison with the initial NaX. S<sub>II</sub> is practically fully occupied in both of the lattice atoms in original evacuated NaX and in the same sample after chemisorption of methyl iodide. We observed serious changes in the distribution of the lattice elements after chemisorption of methyl ions. These changes were detected not only in occupation

factors but sometimes also in coordinates of Na<sup>+</sup> cations. Our results (in Table 2) are well in line with these findings of the other authors<sup>1,2,3,4</sup>). For NaLSX we observed in addition another effect resulting from the influence of chemisorbed species on the geometry. This effect was associated with some distortion of cubooctahedra caused probably by chemisorbed species together with associated cation displacement.

*This research has been supported by GA ČR grant No. GA 202/03/0981 and by MŠMT grant No. MSM210000021.*

- [1] W.J. MORTIER, J.SAUER, J.A. LERCHER, H. NOLLER: J.Phys. Chem. 88, 1984, pp. 905-10.
- [2] Z. JIRÁK, S. VRATISLAV, V. BOSÁČEK: J.Phys. Chem. Solids 41, 1980, pp. 1098-95.
- [3] S. VRATISLAV, M. DLOUHÁ, V. BOSÁČEK: Physica B 276-278 2000 pp. 29-31.
- [4] S. VRATISLAV, M. DLOUHÁ, V. BOSÁČEK: Applied Physics A 74 2002 pp. 1320-21.

## T11 - P205

### ESTIMATES OF THE UNCERTAINTY OF LATTICE PARAMETERS REFINED FROM NEUTRON POWDER DIFFRACTION DATA

Burkhard Peplinski<sup>a</sup>, Daniel M. Toebbens<sup>b</sup>, Winfried Kockelmann<sup>c</sup>, Richard Ibberson<sup>c</sup>

<sup>a</sup> Federal Institute for Materials Research and Testing (BAM),  
Richard-Willstätter-Str. 11, D-12489 Berlin, Federal Republic of Germany

<sup>b</sup> Hahn-Meitner-Institute (HMI), BENSC, SF2

Glienicker Str. 100, D-14109 Berlin, Federal Republic of Germany

<sup>c</sup> ISIS facility, Rutherford Appleton Laboratory (RAL), Chilton, Didcot, OX11 0QX, UK

Lattice parameter refinements from neutron diffraction (ND) data may be preferred to those from diffraction data collected with conventional X-rays or synchrotron radiation, for example if investigations on coarse-grained powders or bulk samples, with volumes of up to several cubic centimetres, are meant to be representative for the *whole* specimen. For these kind of analyses ND takes advantage of the high penetration of neutrons for most elements (isotopes), allowing them to simultaneously probe the whole volume of a thick specimen with nearly no attenuation. Furthermore, with ND the observed intensities of Bragg reflections are averaged over a larger number of crystallite *orientations* than the high-resolution modes of the conventional X-ray or synchrotron radiation techniques usually allow. This is a consequence of the large equatorial and axial divergence normally employed in constant wavelength ND beam optics and of the wide wavelength spectrum and the large acceptance angles of the detector banks used in time-of-flight (ToF) ND. From the metrological point of view the following three aspects of the uncertainty of measurement are especially relevant:

1. If the lattice parameter refinement is carried out by the Rietveld method or by any other whole pattern technique, then the only available measures of the uncertainty of the refined lattice parameters are the estimated standard

deviations (e.s.d.s) calculated by the full pattern fitting program. However, e.s.d.s are measures of precision rather than of accuracy and these two terms must not be confused.

2. e.s.d.s calculated by many Rietveld programs are not reliable measures of the 'probable errors', because, in many cases, they are systematically too small, due to 'serial correlation'. Therefore, uncorrected e.s.d.s are not only no measure of accuracy, but even no reliable measure of the precision of refined lattice parameters. The e.s.d.s are calculated under the assumption that the values in the difference curve are independent observations. However, adjacent individual points in the difference curve are not independent but correlated by the used profile function. This correlation depends on the size of the 2 steps used for data collection and evaluation. A formula for estimating the corrections that should be applied to the e.s.d.s has been given by Berar and Lennan [1] who established that e.s.d.s calculated by Rietveld programs *without* consideration of serial correlations are often too small by a factor of approximately two. Therefore, at the 65% confidence level, the *probable* errors are calculated from the uncorrected e.s.d.s by multiplying the latter by a factor of about two. Consequently, the U<sub>95%</sub> uncertainties of measurement at the 95% confidence level are calculated by multiplying the uncorrected e.s.d.-values by a factor of about *four*.



3. Bragg's law involves a 100% correlation between the  $d$ -values (and therefore the lattice parameters) of a crystallographic phase and the wavelength of the diffracted radiation.

Thus for any assumed value of the wavelength another set of lattice parameters results, whereas the agreement indices and the e.s.d.s *remain the same*. Since for *all* neutron diffractometers the wavelength is not known *per se*, as would be the case with characteristic X-ray radiation, even under the idealising assumption of the complete absence of any systematic errors from the model and from the observed data the lattice parameters are completely *indeterminate*. Therefore, a determination of accurate lattice parameters by constant wavelength ND or ToF ND *necessarily* includes calibration procedures with reference materials that have lattice parameters certified for a given temperature by *independent* analytical techniques. The propagation of the error resulting from the calibration procedure *should* be considered in the estimation of the total uncertainty of the lattice parameters of the actual sample under investigation! Consequently, in the case that the calibration procedure as well as the analysis of the actual sample are carried out by the Rietveld method or any other whole pattern technique the  $U_{95\%}$  uncertainties of the final analysis results can be as large as the *eight-fold* of the uncorrected e.s.d.s from a single refinement!

Further aspects of the uncertainty of measurement (e.g. line shifts due to absorption or the question about preferences for the methods of internal or external standard) have to be analysed separately for each of the following three types of ND instruments:

a. High-resolution powder ToF-ND instruments, see e.g. [2].

b. High-resolution powder diffractometers for monochromatic neutrons, equipped with parallel collimators placed in front of the detectors and restricting the equatorial divergence of the diffracted beam (prototype: D1A and D2B at the ILL, see e.g. [3]).

c. Powder diffractometers for monochromatic neutrons in Debye-Scherrer-geometry with one (or several) position-sensitive detector(s) providing resolution in the equatorial plane.

The determination of accurate lattice parameters through the refinement of diffraction data collected with any type of these instruments requires highly accurate mathematical modelling of the observed diffraction line profiles. For a constant wavelength ND instrument of type

b this can be achieved by the 'fundamental parameter approach' which combines the individual contributions to the reflection profile by convolution integrals. This leads to the following writing of Bragg's law:

$$d_{hkl} = 0.5 \lambda_{\text{eff}} \sin\left\{ \lambda_{\text{obs}} \left[ \frac{EPS_{1,\text{eff}}}{f_{\text{ax.div approx.}}(R, h_d, h_s, FWHM, \cot 2\theta)} \right] \right\} \quad (1)$$

with  $\lambda_{\text{eff}}$  = effective value of the wavelength;  $\lambda_{\text{obs}}$  = observed halved diffraction angle;  $EPS_{1,\text{eff}}$  = effective value of the zero correction for the detector bank;  $f_{\text{ax.div approx.}}$  = axial divergence;  $R$  = diffractometer radius;  $h_d$  = effective height of the detector;  $h_s$  = effective height of the specimen;  $FWHM$  = contribution to the reflection profile caused by the real structure of the specimen;  $f_{\text{ax.div approx.}}$  is the 'axial divergence correction function' which can be determined only approximately due to strong correlations between some of the parameters.

By differentiating equation (1) a formula for the uncertainty of refined lattice parameters can be derived that contains a number of individual contributions, not all of which are additive. An analogous formula can be derived for ToF-ND. By the analysis of the individual contributions and by taking into account the results of the proficiency testing carried out at several ND instruments (see e.g. [4-5]) it can be shown that the lattice parameters of cubic, tetragonal, hexagonal and orthorhombic materials can be refined in the metric system and at the 95% confidence level with a relative accuracy of  $a_i/a_i \approx 2 \cdot 10^{-5}$  using a high-resolution multi-collimator/multi-detector powder diffractometer for monochromatic neutrons or a dedicated high-resolution ToF-ND instrument.

The present study is based on the analysis of data published by a number of laboratories as well as on experimental results of the authors. It facilitates the statistically sound interpretation of differences between lattice parameters refined on the same sample using different ND instruments.

1. Berar J.F., Lennan P. (1991) J. Appl. Cryst. **24**, 1-5.
2. David W.I.F. et al. (1986) Mater. Sci. Forum **9**, 89-101.
3. Hewart A.W. (1986) Mater. Sci. Forum **9**, 69-79.
4. Toebbens D.M. et al. (2001) Mater. Sci. Forum **378-381**, 288-293.
5. Kockelmann W. et al. (2000) Mater. Sci. Forum **321-324**, 332-337.



T11 - P206

## NEUTRON DIFFRACTION STRUCTURE STUDY OF BOROSILICATE BASED MATRIX GLASSES

M. Fábrián<sup>1</sup>, E. Sváb<sup>1</sup>, Gy. Mészáros<sup>1</sup>, L. Kőszegi<sup>1</sup>, L. Temleitner<sup>1</sup>, E. Veress<sup>2</sup>

<sup>1</sup> Research Institute for Solid State Physics and Optics, H-1525, Budapest POB 49, Hungary

<sup>2</sup> Babeş-Bolyai University, Faculty of Chemistry, 11 Arany János St., RO-3400 Cluj, Romania

Borosilicate glasses assure the safe immobilization of most radionuclides even in large quantities, their properties being highly adaptive as concerns the nature, quantity and activity level of the radioactive species present in the waste [1-5]. Therefore the study of borosilicate glasses is of significant current interest as suitable materials for isolating host media for radioactive waste materials.

We have performed structure investigation by means of neutron diffraction on a newly synthesized borosilicate glass system. The matrix glass with general composition of  $65\text{SiO}_2 \cdot 25\text{Na}_2\text{O} \cdot 5\text{BaO} \cdot 5\text{B}_2\text{O}_3$  was doped with  $\text{ZrO}_2$  to increase the stability, and with  $\text{CeO}_2$  to simulate radioactive  $\text{PuO}_2$ . As  $\text{Ce}$  and  $\text{Pu}$  coordination is similar in complex oxide environments, it can be expected that  $\text{Pu}$  coordination will be properly simulated by  $\text{Ce}$  addition in the host glasses. The samples were prepared by melting in platinum crucible at 1300-1450 °C, working in atmospheric conditions. The melt was quenched by pouring on an inox plate. We have investigated two series of samples with the general composition of  $(65-x)\text{SiO}_2 \cdot 25\text{Na}_2\text{O} \cdot 5\text{BaO} \cdot 5\text{B}_2\text{O}_3 \cdot x\text{ZrO}_2$  and  $\{(65-x)\text{SiO}_2 \cdot 25\text{Na}_2\text{O} \cdot 5\text{BaO} \cdot 5\text{B}_2\text{O}_3 \cdot x\text{ZrO}_2 + 10\text{CeO}_2\}$  0 ≤ x ≤ 5 (in mole%).

Neutron diffraction measurements were carried out at the 10 MW Budapest research reactor using the 'PSD' [6] and 'MTEST' [7] neutron diffractometers. Powder samples were prepared by milling in an agate mill of the poured and quenched glasses. Despite of the great hydrolytic stability of the samples, the first few experiments revealed their tendency to superficially adsorb  $\text{H}_2\text{O}$ . Atmospheric humidity caused a surface swelling (hydrolysis) of the air-kept samples, and the hydrogen contained by the hydrolysed layer produced great incoherent scattering, causing difficulties in the data treatment. The samples were dried at 120 °C for 4 hours under vacuum conditions, which proved to be completely sufficient to obtain neutron diffraction pattern adequate for data treatment.

All samples from the  $(65-x)\text{SiO}_2 \cdot 25\text{Na}_2\text{O} \cdot 5\text{BaO} \cdot 5\text{B}_2\text{O}_3 \cdot x\text{ZrO}_2$  series were found to be amorphous, while addition of  $\text{Ce}$  to the matrix composition lead to partial crystallization of the glass. Amorphous phase could be stabilized by increasing the  $\text{Zr}$ -content. Specimens of the  $(65-x)\text{SiO}_2 \cdot 25\text{Na}_2\text{O} \cdot 5\text{BaO} \cdot 5\text{B}_2\text{O}_3 \cdot x\text{ZrO}_2 + 10\text{CeO}_2$  series were found to be partly crystalline for x ≥ 3, while they were amorphous for x ≤ 4.

The structure factor,  $S(Q)$  of the amorphous specimens was determined from the measured pattern using correction and normalization procedure. For data treatment both the traditional direct Fourier-transformation, and the reverse Monte Carlo (RMC) simulation [8] method were applied. For the RMC starting model a disordered atomic configura-

tion was build up. The convergence of the RMC calculation was good inspite of the extremely high number of simulated parameters (about 600), and the final fit matched very well the experimental structure factors as it shown in Figs. 1/a and 2/a, as representatives for a  $\text{Zr}$  containing sample and for a  $\text{Zr}$  and  $\text{Ce}$  containing specimen, respectively. The fit consists of minimizing the squared difference between the experimental and calculated structural factors by moving atoms randomly.

We could successfully calculate the most important partial atomic pair correlation functions,  $g(r)$  for all specimens. The different atomic distances of the glass network were calculated, i.e. the first neighbour  $\text{Si-O}$  and  $\text{B-O}$  distances at 1.4 and 1.7 Å, respectively. The  $\text{Si-O}$  and  $\text{B-O}$  pair correlation functions contributing to the 1st coordination shell are shown in Fig. 1/b,c and the  $\text{O-O}$ ,  $\text{O-Na}$  and  $\text{O-Zr}$   $g(r)$ 's contributing to the 2nd coordination sphere are collected in Fig. 1/d-f for the  $62\text{SiO}_2 \cdot 25\text{Na}_2\text{O} \cdot 5\text{BaO} \cdot 5\text{B}_2\text{O}_3 \cdot 3\text{ZrO}_2$  glass. For the  $60\text{SiO}_2 \cdot 25\text{Na}_2\text{O} \cdot 5\text{BaO} \cdot 5\text{B}_2\text{O}_3 \cdot 5\text{ZrO}_2 + 10\text{CeO}_2$  (mol%) sample the results of the RMC simulation are collected in Fig. 2 showing the contributing  $g(r)$ 's to the 2nd atomic sphere.

From the RMC simulation of the neutron diffraction data we have obtained the partial atomic pair correlation functions for these multi-component glasses, making possible to determine first neighbour atomic distances and coordination numbers. A slight dependence of the parameters on the  $\text{Zr}$  and  $\text{Ce}$  concentration was analysed and will be presented. Addition of  $\text{Zr}$  proved to stabilize the amorphous structure, even  $\text{Zr}$  can compensate the crystallizing effect of  $\text{Ce}$ .

It was established that the basic network configuration is the same of the investigated samples, making them suitable for radioactive waste material storage.

### Acknowledgement

This study was supported by the Hungarian Research Grant OTKA T-42495.

1. Inman, J.M., Houde-Walter, S.N., McIntyre, B.L., Liao, Z.M., Parker, R.S. and Simmons, V. (1996) *Journal of Non-Crystalline Solids* 194, 85
2. Donald, I.W., Metcalf, B.L. and Taylor, R.N.j. (1997) *Journal of Material and Science* 32, 5851
3. Li, H., Vienna, J.D., Hrma, P., Schweiger, M.J., Smith, D., Gong, M., (1996) *Ceramic Transactions*, 72, 399-408.
4. MacFarlane, A. (1998) *Science & Global Security*, 7, 271-309.
5. Orlhac, X., Fillet, C., and Phalippon, J. (1998) *Scientific Basis for Nuclear Waste Manag.*, 556, 263-2

6. Sváb, E., Deák, F. and Mészáros, Gy.(1996) *Mater. Sci. Forum.* **228-231**, 247- 252.  
7. Kőszegi, L. *Journal on Neutron Research* (2001) **9**, 381-384.

8. McGreevy, R.L. and Pusztai, L. (1988) *Molec. Simul.* **1**, 359-367.

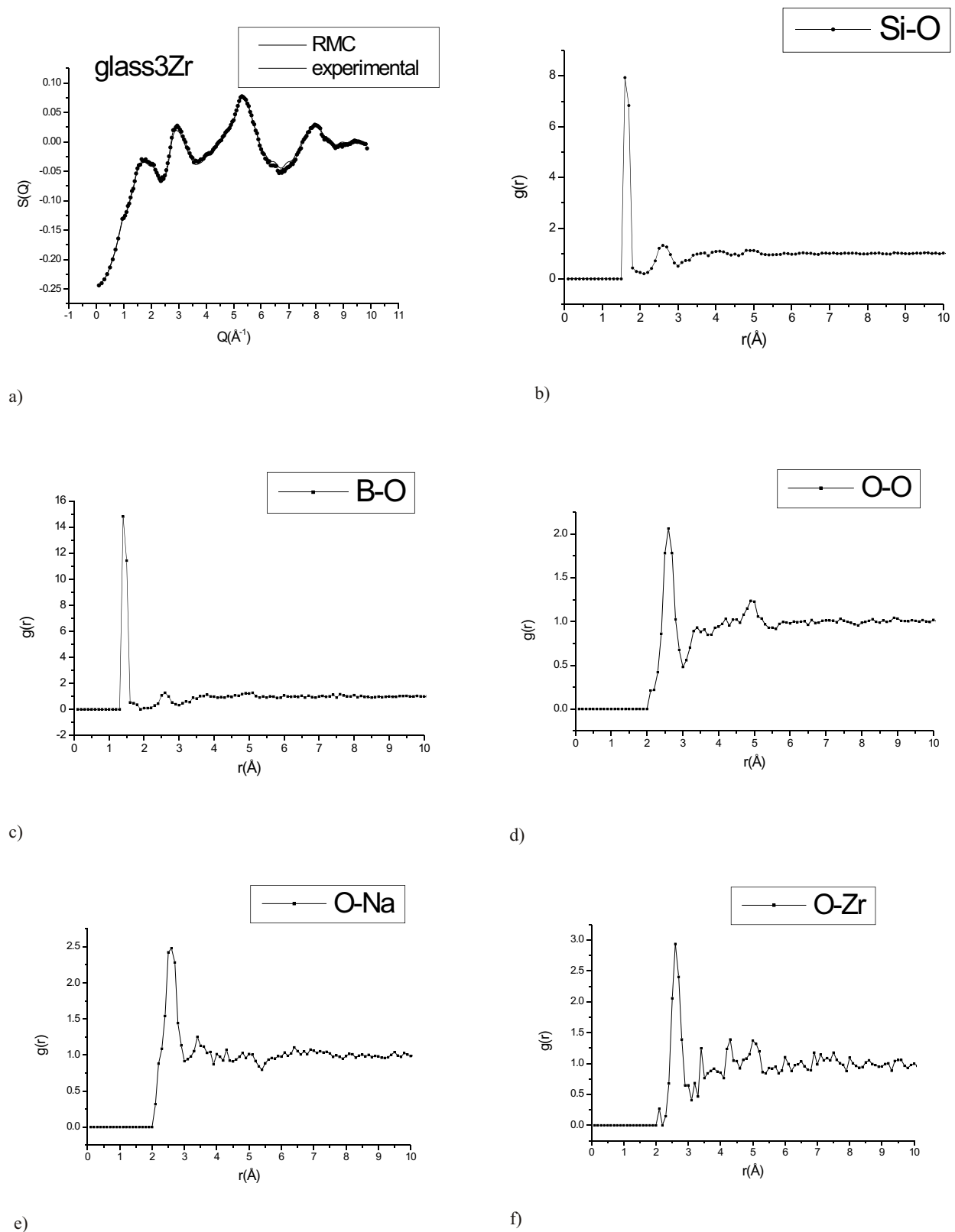


**Figure 1.** Neutron diffraction spectrum and RMC simulation of  $62\text{SiO}_2 \cdot 25\text{Na}_2\text{O} \cdot 5\text{BaO} \cdot 5\text{B}_2\text{O}_3 \cdot 3\text{ZrO}_2$  glass: a/ measured pattern and RMC simulation b/ Si-O c/ B-O d/ O-O e/ O-Na and f/ O-Zr partial pair correlation functions

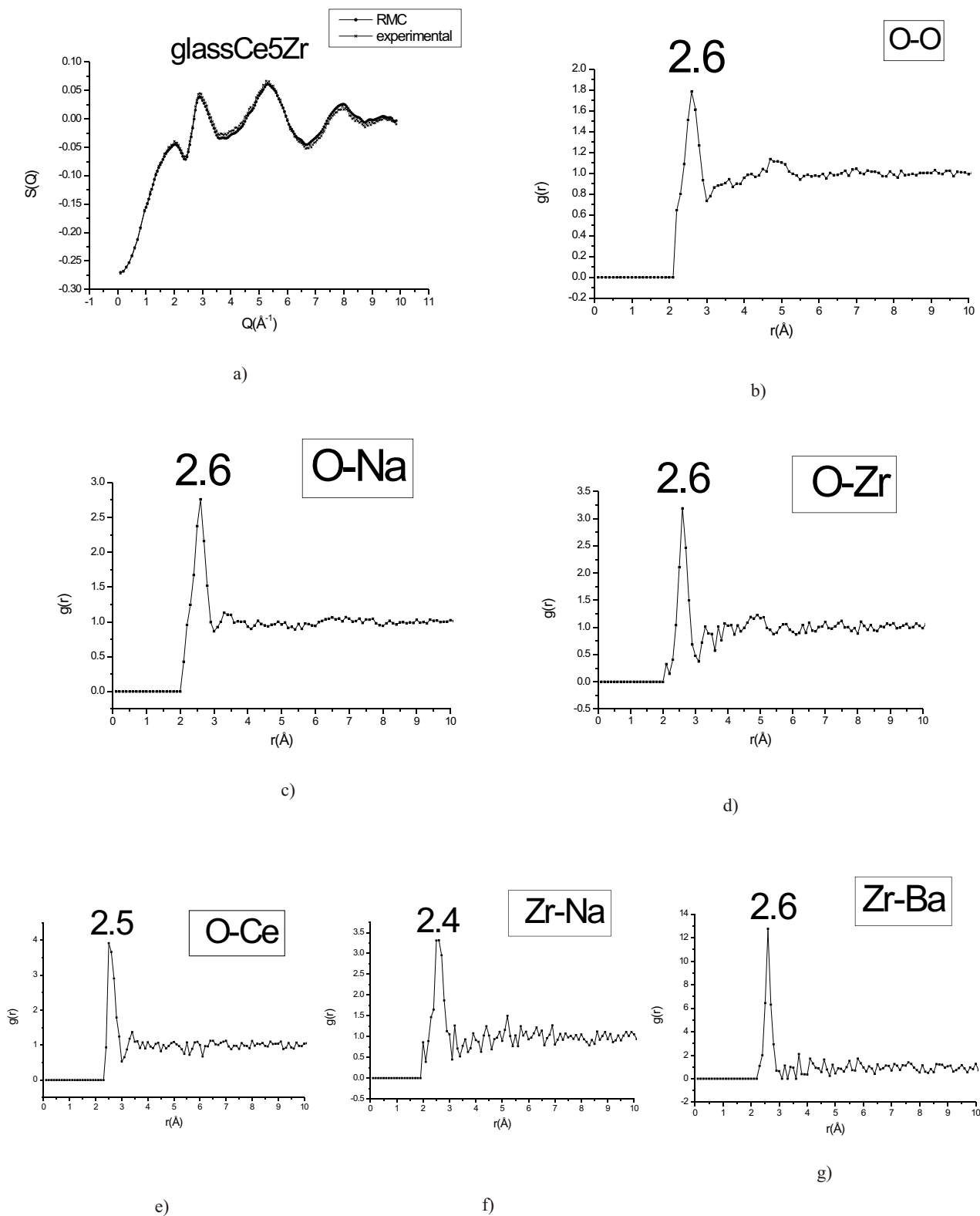


**Figure 2.** Neutron diffraction spectrum and partial pair correlation functions from RMC simulation of  $60\text{SiO}_2 \cdot 25\text{Na}_2\text{O} \cdot 5\text{BaO} \cdot 5\text{B}_2\text{O}_3 \cdot 5\text{ZrO}_2 + 10\text{CeO}_2$  (mol%) glass: **a/** measured  $S(Q)$  and RMC simulation **b/** O-O **c/** O-Na **d/** O-Zr **e/** O-Ce **f/** Zr-Na and **g/** Zr-Ba